Fate of an impurity strongly interacting with a thermal Bose gas

Jiří Etrych¹, Sebastian J. Morris¹, Simon M. Fischer¹, Gevorg Martirosyan¹, Christopher J. Ho¹, Moritz Drescher², Manfred Salmhofer², Zoran Hadzibabic¹, Tilman Enss², and Christoph Eigen^{1,*}

¹ Cavendish Laboratory, University of Cambridge, J. J. Thomson Avenue, Cambridge CB3 0HE, United Kingdom

² Institut für Theoretische Physik, Universität Heidelberg, 69120 Heidelberg, Germany

We spectroscopically study mobile impurities immersed in a homogeneous bosonic bath (a box-trapped Bose gas), varying the bath temperature and the strength of impurity-bath interactions. We compare our results to those for a quasipure Bose–Einstein condensate (BEC), and find that for strong impurity-bath interactions, the spectra narrow with increasing temperature, while the impurity energy shift is suppressed. Near the critical temperature for condensation, many-body effects still play an important role, and only for a nondegenerate bath, the system approaches the classical Boltzmann-gas behavior. The key spectral features are reproduced within the theory of an ideal Bose polaron.

An impurity immersed in a quantum bath is a fundamental setting in many-body physics that, in spite of its apparent simplicity, features complex emergent behavior. A key simplification often lies in treating the impurities dressed by the excitations of the bath as polaron quasiparticles. This notion originates from descriptions of electrons moving through a polarizable crystal [1, 2], but nowadays extends to numerous scenarios in condensed matter physics and beyond [3, 4].

In cold-atom experiments, impurity physics can be studied in highly imbalanced two-component mixtures, where the minority component acts as impurities and the majority component as the bath [5–8]. A key advantage of these experiments is the high degree of tunability: the bath density n and temperature T are readily controllable, and the strength and sign of the impurity-bath interactions, characterized by the s-wave scattering length a, can be tuned using Feshbach resonances. In the high-temperature regime, the mixture can be described as a classical Boltzmann gas, and the thermal de Broglie wavelength $\lambda \propto 1/\sqrt{T}$ sets the relevant interaction parameter a/λ . Instead, in the low-temperature regime, the impurity behavior depends on the quantum statistics of the bath, and is generally governed by the interaction parameter $k_n a$, where $k_n = (6\pi^2 n)^{1/3}$ [5–8].

For a fermionic bath, long-lived attractive and repulsive polaron quasiparticles exist for temperatures well below the Fermi temperature [9, 10], but the quasiparticle description breaks down as T is increased [11]. The situation is more intricate for a bosonic bath: in the limit of vanishing intrabath interactions, there is no overlap between the ground state of the system with and without the impurity; this is known as the bosonic orthogonality catastrophe [12, 13]. When the bath is weakly repulsive and the reduced temperature $T/T_c \ll 1$, where T_c is the critical temperature for Bose-Einstein condensation, well-defined attractive and repulsive polarons exist at sufficiently low a [14, 15], but in the strongly interacting regime the quasiparticle picture breaks down and the spectra are intrinsically broad [16]. The fate of the system at finite T, including the effect of the BEC phase transition, is subject to ongoing theoretical debate [17-22], with previous experiments limited to strong attractive interactions [23]. Furthermore, in contrast to fermions, strongly interacting bosons are unstable due to three-body loss (due to the absence of Pauli blocking), making it challenging to investigate their equilibrium properties.

In this Letter, we study impurities injected into a box-trapped Bose gas, mapping out the impurity spectrum across the strong-coupling regime for different T/T_c . We compare our measurements to those obtained for a quasipure BEC [16], and find that the spectral shift in a thermal gas is suppressed compared to the BEC and, counterintuitively, near unitarity the spectra narrow with increasing T. Near T_c , the spectra retain clear many-body character, with three key signatures: (i) the spectral shifts and widths are set by the energy scale $E_n = \hbar^2 k_n^2/(4m_r)$, where m_r is the reduced mass of an impurity and a bath atom, (ii) the attractive branch extends across the resonance, and (iii) the spectral width is asymmetric in $1/(k_n a)$, reaching a maximum value for $1/(k_n a) \approx 0.4$. For higher T/T_c , the system approaches the Boltzmann-gas regime: the attractive and repulsive spectral branches connect across the resonance, and the width is symmetric in λ/a , reaching its maximum (unitarity-limited) value at $\lambda/a \approx 0$. Throughout, we compare our results to bosonic functional determinant approach (FDA) calculations for an ideal Bose polaron [22], finding excellent qualitative agreement.

Our experiments are performed using a gas of ³⁹K atoms in an optical box trap [24–26] of volume $V = 3.3(7) \times$ $10^4 \,\mu\text{m}^3$, initially spin-polarized in the $|F, m_F\rangle = |1, -1\rangle$ state, here denoted as | † >. We prepare thermal samples with T/T_c up to ≈ 4 , varying both the temperature and the density of the sample [27]. As illustrated in Fig. 1(a) and following [16], we perform rf injection spectroscopy by coupling $|\uparrow\rangle$ to the $|1,0\rangle = |\downarrow\rangle$ (impurity) state with long, weak pulses [28] of frequency $\omega/(2\pi)$, and measure the fraction of atoms transferred to ||) as a function of the detuning $\delta/(2\pi)$ from the bare atomic transition frequency $\omega_0/(2\pi)$, such that $\omega = \omega_0 + \delta$. We tune the impurity-bath interactions by changing the magnetic field in the proximity of the interstate Feshbach resonance at $B_{res} = 526.16(3) \,\text{G} \,[16]$; the intrabath interactions are always weakly repulsive, with the intrastate $(|\uparrow\rangle - |\uparrow\rangle)$ scattering length $a_b \approx 20a_0$.

The theoretical spectra are calculated within the model of an ideal Bose polaron (an infinitely heavy impurity in a noninteracting Bose gas) [22, 29], which, however, applies only approximately to our experiment; in particular, it neglects the motional degrees of freedom of a finite-mass impurity and short-range bath correlations due to intrabath repulsion and/or three-body physics. To compare to this theory, we assume that the finite mass only affects the absolute energy

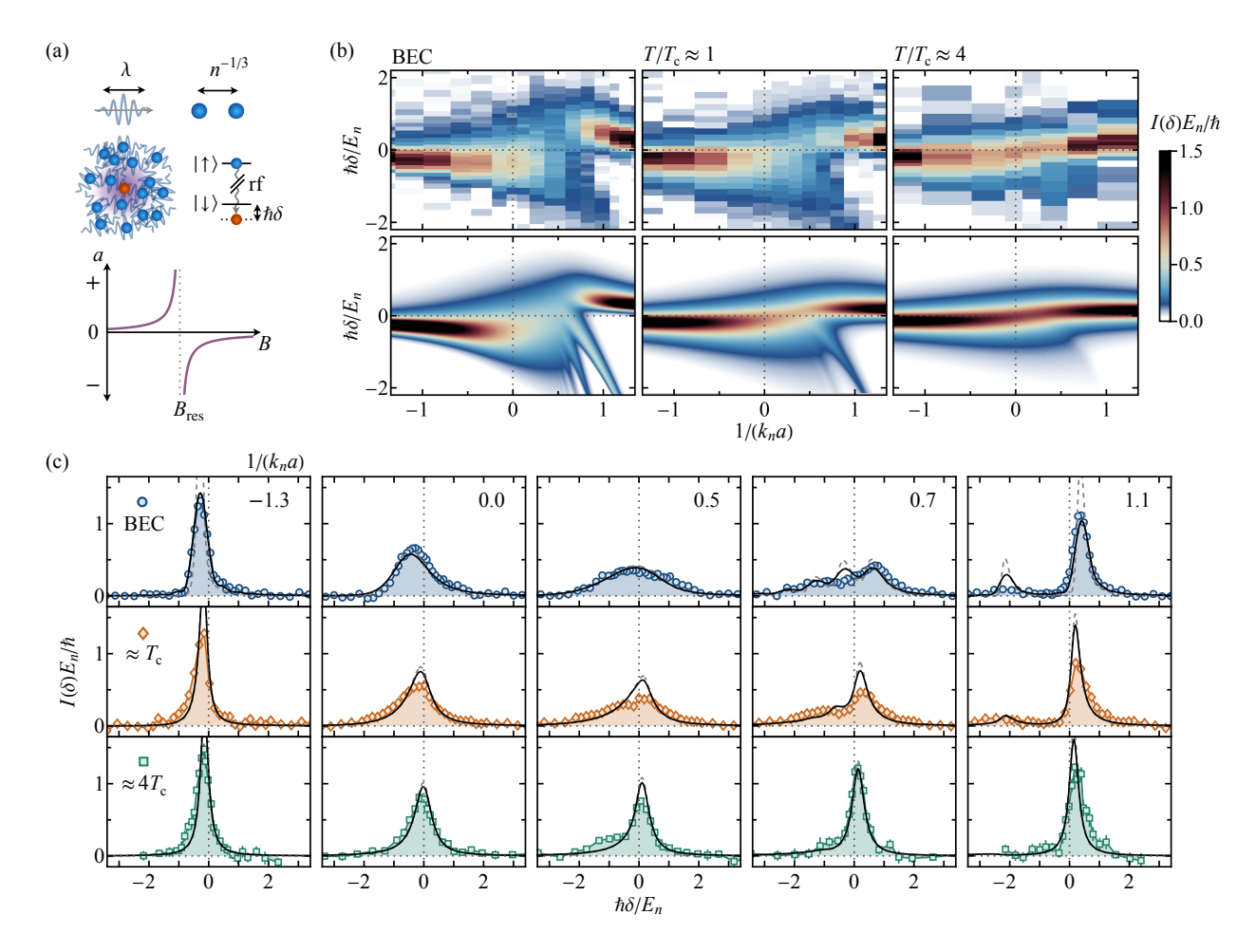


FIG. 1. Injection spectroscopy of impurities in a bosonic bath. (a) We start with a spin-polarized Bose gas, with tuneable thermal wavelength $\lambda \propto 1/\sqrt{T}$ and interparticle separation $n^{-1/3} \propto 1/k_n$, set by the gas temperature T and density n (top). We use rf pulses of variable detuning δ to inject a small fraction of impurities, mapping out the spectral response $I(\delta)$ (middle). The impurity-bath interactions, characterized by the interstate scattering length a, are tuneable by changing the magnetic field B in the vicinity of a Feshbach resonance (bottom). (b) Experimental impurity spectra (top) and ideal-polaron calculations (bottom) in the strong-coupling regime for three different baths: an initially quasipure Bose–Einstein condensate (BEC) with $n \approx 12 \mu m^{-3}$ [16] (left), a Bose gas near the critical temperature for condensation T_c [$T \approx 130$ nK, $n \approx 5 \mu m^{-3}$] (middle), and a thermal gas at $T/T_c \approx 4$ [$T \approx 260$ nK, $n \approx 1.7 \mu m^{-3}$] (right). (c) Example experimental (symbols) and theoretical (solid lines) injection spectra for our three bath temperatures at different $1/(k_n a)$ (left to right), corresponding to vertical cuts through the panels in Fig. 1(b). In the strong-coupling regime, the spectral response narrows with increasing T. Note that we have convolved the theoretical spectra with the residual Fourier broadening (arising from the finite rf-pulse duration); for comparison, the unconvolved spectra are shown as dashed lines.

scale $(E_n \propto 1/m_r)$, and we set m_r to our value m/2, where m is the atom mass.

In Fig. 1(b), we show an overview of our main results, the injection spectra $I(\delta)$ in both experiment (top) and theory (bottom), for various $1/(k_n a)$ and three different baths: an initially quasipure BEC ($T/T_c < 0.1$), a Bose gas near criticality $(T/T_c \approx 1)$, and a thermal gas $(T/T_c \approx 4)$ [30]; the spectra are normalized such that $\int I(\delta)d\delta = 1$ and for the BEC comparison, we use $T/T_c = 0.15$ in the theory [31]. For the BEC case, the attractive branch extends to $1/(k_n a) > 0$ and for $1/(k_n a) > 0.5$, both the attractive $(\delta < 0)$ and the repulsive $(\delta > 0)$ branches are clearly resolved. For $T/T_c \approx 1$, the spectral shifts are generally suppressed compared to the BEC case. Across the resonance, spectral weight is more continuously transferred between the two branches, but the attractive branch also still extends to $1/(k_n a) > 0.5$. For $T/T_c \approx 4$, the spectral shift near unitarity is fully suppressed, the two branches connect across the resonance, and there is little attractive-branch spectral weight for $1/(k_n a) > 0$; in the high-T limit, the only relevant attractive state is the interstate dimer, which has little overlap with our initial free-atom states.

The ideal-polaron calculations reproduce the qualitative features of the experimental spectral functions, with the exception of the attractive branch at $1/(k_n a) > 0.5$, where the theory predicts multiple well-separated peaks, while a single broad feature is observed in the experiment. However, this regime is known to be pathological in this model and short-range physics needs to be included for a correct theoretical description of the lower-lying attractive states [32]; a quantitative understanding of these states and calculation of the full spectral function remains a challenge (see also [33]).

In Fig. 1(c), we show example spectra for our three T/T_c at different $1/(k_n a)$. The temperature effects are the most striking in the range $0 \lesssim 1/(k_n a) \lesssim 0.7$, where the BEC spectra are the broadest. For $T/T_c \approx 1$, the widths of the

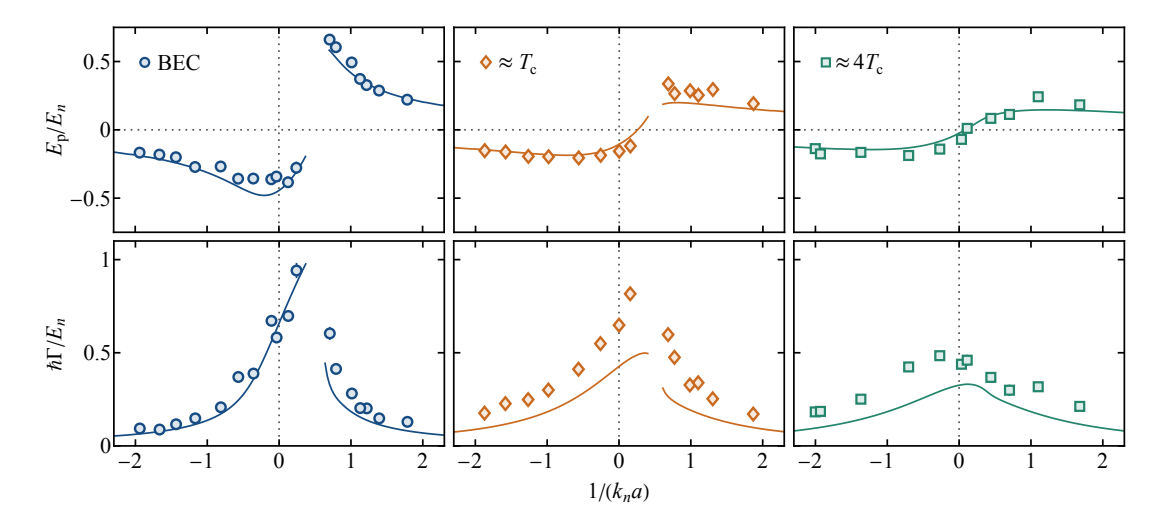


FIG. 2. Spectrum mode E_p/E_n (top) and half-width-at-half-maximum $\hbar\Gamma/E_n$ (bottom) versus $1/(k_n a)$ for our three different baths (increasing T/T_c left to right); the solid lines show the corresponding ideal-polaron FDA calculations. We refrain from extracting E_p and Γ for the attractive branch for $1/(k_n a) \gtrsim 0.3$.

spectra are comparable to or smaller than for the BEC, and for $T/T_{\rm c}\approx 4$ the spectra are significantly more narrow. This behavior is notably different compared to the temperature evolution of spectral features in cold Fermi gases, where broadening with increasing temperature is generally observed, and only at temperatures above the Fermi temperature the spectra slowly narrow as $1/\sqrt{T}$ due to unitarity-limited collisions [11, 34].

We characterize the spectra by their peak position E_p/E_n and half-width-at-half-maximum $\hbar\Gamma/E_n$ [35], and in Fig. 2, we plot these extracted quantities as a function of $1/(k_na)$. For $T/T_c \approx 1$, the measured $|E_p|/E_n$ values are significantly lower than for the BEC, but they change only slowly between $T/T_c \approx 1$ and 4. The width at $T/T_c \approx 1$ shows the same asymmetric dependence on $1/(k_na)$ as the BEC data (with a maximum at $1/(k_na) > 0$), but it becomes more symmetric for $T/T_c \approx 4$, with the maximum value instead reached at $1/(k_na) \approx 0$.

While the BEC data are well captured by the idealpolaron theory (solid lines) [31], the agreement is only qualitative for the thermal baths; in particular, the experimental widths are about 50% larger compared to the theoretical ones, and for $T/T_c \approx 1$, the experimental E_p/E_n of the repulsive branch is about 30% larger than the theory. These differences could arise for at least two reasons. First, the ratio of thermal and interaction energy scales is intrinsically different in the ideal-polaron model (where $k_B T_c \approx 0.88 E_n$) and our mobile-impurity case (where $k_B T_c \approx 0.44 E_n$), leading to more significant suppression of (many-body) interaction effects in the theory compared to the experiment. Secondly, for rf injection starting from a spin-polarized thermal Bose gas, one expects the spectral shifts to be enhanced due to bosonic bunching, which arises from coherence between the impurity and bath states. In the mean field limit (at low a), one expects $E_{\rm mf} = 2\pi\hbar^2 \alpha na/m_{\rm r}$ with $\alpha = 2$ (compared to $\alpha = 1$ for a pure BEC) [36, 37], and such enhancement could still play a role in the strongly interacting regime. However, note that even for low a, we curiously find α closer to 1 [31], and understanding the role of coherence in injection experiments remains a challenge for the future.

Finally, we study the crossover to the classical Boltzmann-gas regime, in which only two-body effects are relevant and one can (to a good approximation) obtain the spectral shift and width, respectively, from the real and imaginary part of the complex energy $\Sigma = E_{\rm p} - i\hbar\Gamma = -2\pi\hbar^2\alpha nf(a)/m_{\rm r}$, where $f(a) = \langle -a/(1+ika)\rangle_{\rm th}$ is the thermally averaged two-body scattering amplitude [31]. In this case, the natural interaction parameter is a/λ , where $\lambda = \sqrt{2\pi\hbar^2/(mk_{\rm B}T)}$, and the natural energy scale $E_0 = E_{\rm mf}\lambda/a = 2\pi\hbar^2\lambda\alpha n/m_{\rm r}$. Near the resonance, the interactions become unitarity-limited: at $\lambda/a = 0$, the scattering amplitude and Σ become purely imaginary, the spectral shift is zero, and the width is maximal.

In Fig. 3, we compare our measurements to this universal high-T prediction (solid line), plotting E_p/E_0 versus λ/a for our three bath temperatures; we experimentally determine E_0 from the slope of E_p versus a in the mean-field regime $(a \ll \lambda)$ [31]. The E_p data approach the theory only for our

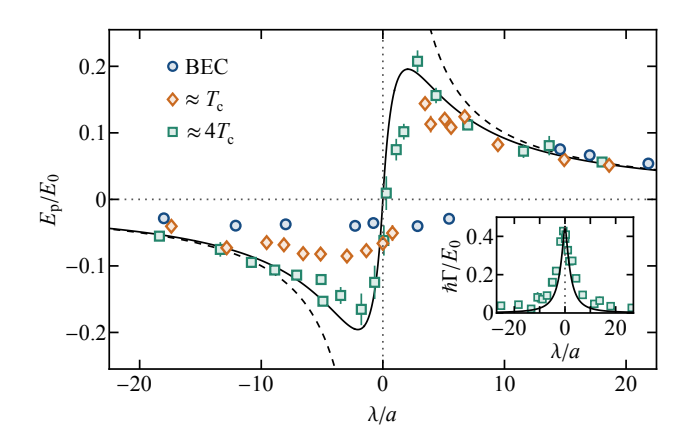


FIG. 3. Crossover to the Boltzmann-gas regime. The main panel shows E_p/E_0 versus λ/a , where $E_0=E_{\rm mf}\lambda/a=2\pi\hbar^2\lambda\alpha n/m_{\rm r}$; to include the BEC data, we used the estimated initial $T\approx 10\,{\rm nK}$ [38]. The inset shows $\hbar\Gamma/E_0$ versus λ/a for $T/T_c\approx 4$. The solid lines show the universal two-body prediction valid for $T/T_c\gg 1$, while the dashed line shows the mean-field prediction $E_p=E_{\rm mf}$.

highest temperature $T/T_c \approx 4$; here the width $\hbar\Gamma/E_0$ also agrees with the theory for $\lambda/a \approx 0$, but is systematically higher away from unitarity (see inset).

Our highest temperature corresponds to a phase-space density $n\lambda^3 \approx 0.3$, meaning that the two-body theory becomes valid only for an essentially nondegenerate bath, while for a degenerate bath near T_c (where all three principal lengthscales a, λ , and $1/k_n$ are comparable in magnitude) many-body effects are significant [39].

In conclusion, we have investigated the spectral response of impurities strongly interacting with a thermal bosonic bath, revealing the importance of many-body effects in the degenerate regime, and studying the crossover to the classical Boltzmann-gas regime with unitarity-limited scattering. The comparison of our thermal-bath spectra with previous measurements for an impurity in a quasipure BEC highlights the conceptual differences between bosonic and fermionic baths: while sharp quasiparticle features emerge at low T in the fermionic case, the bosonic spectral response is intrinsically broad at strong interactions. The qualitative observations are well captured in the ideal-polaron theory, which neglects impurity motional degrees of freedom and short-range bath correlations, but crucially includes the macroscopic deformation of the bath.

In the future, it would be interesting to extend our study to the case of light impurities, where Efimov physics is predicted to play a more important role [40, 41], or to systems with stronger intrabath repulsion, where the quasiparticles are expected to be more well-defined [13] and, furthermore, the thermal bath becomes hydrodynamic [42]. Our work also motivates the development of novel theoretical approaches that capture the effect of short-range bath correlations [especially relevant for the attractive branch at $1/(k_n a) > 0$] at arbitrary T.

We thank Martin Gazo for discussions and comments on the manuscript. The Cambridge work was supported by EPSRC [Grant Nos. EP/P009565/1 and EP/Y01510X/1], ERC [UniFlat], and STFC [Grants No. ST/T006056/1 and No. ST/Y004469/1]. Z.H. acknowledges support from the Royal Society Wolfson Fellowship. The Heidelberg work was supported by the DFG (German Research Foundation) under Project No. 273811115 (SFB 1225 ISOQUANT) and under Germany's Excellence Strategy EXC2181/1-390900948 (the Heidelberg STRUCTURES Excellence Cluster).

- * ce330@cam.ac.uk
- L. D. Landau, Electron Motion in Crystal Lattices, Phys. Z. Sowjet. 3, 664 (1933).
- [2] S. I. Pekar, Autolocalization of the Electron in an Inertially Polarizable Dielectric Medium, Zh. Eksp. Teor. Fiz 16, 335 (1946).
- [3] A. S. Alexandrov, ed., Polarons in Advanced Materials (Springer, New York, 2008).
- [4] C. Franchini, M. Reticcioli, M. Setvin, and U. Diebold, Polarons in materials, Nat. Rev. Mater. 6, 560 (2021).
- [5] F. Scazza, M. Zaccanti, P. Massignan, M. M. Parish, and J. Levinsen, Repulsive Fermi and Bose Polarons in Quantum

- Gases, Atoms 10, 55 (2022).
- [6] C. Baroni, G. Lamporesi, and M. Zaccanti, Quantum mixtures of ultracold gases of neutral atoms, Nat. Rev. Phys. 6, 736 (2024).
- [7] F. Grusdt, N. Mostaan, E. Demler, and L. A. P. Ardila, Impurities and polarons in bosonic quantum gases: a review on recent progress, Rep. Prog. Phys. 88, 066401 (2025).
- [8] P. Massignan, R. Schmidt, G. E. Astrakharchik, A. İmamoglu, M. Zwierlein, J. J. Arlt, and G. M. Bruun, Polarons in atomic gases and two-dimensional semiconductors, arXiv:2501.09618 (2025).
- [9] A. Schirotzek, C.-H. Wu, A. Sommer, and M. W. Zwierlein, Observation of Fermi Polarons in a Tunable Fermi Liquid of Ultracold Atoms, Phys. Rev. Lett. 102, 230402 (2009).
- [10] C. Kohstall, M. Zaccanti, M. Jag, A. Trenkwalder, P. Massignan, G. M. Bruun, F. Schreck, and R. Grimm, Metastability and coherence of repulsive polarons in a strongly interacting Fermi mixture, Nature 485, 615 (2012).
- [11] Z. Yan, P. B. Patel, B. Mukherjee, R. J. Fletcher, J. Struck, and M. W. Zwierlein, Boiling a Unitary Fermi Liquid, Phys. Rev. Lett. 122, 093401 (2019).
- [12] S. M. Yoshida, S. Endo, J. Levinsen, and M. M. Parish, Universality of an Impurity in a Bose–Einstein Condensate, Phys. Rev. X 8, 011024 (2018).
- [13] N.-E. Guenther, R. Schmidt, G. M. Bruun, V. Gurarie, and P. Massignan, Mobile impurity in a Bose–Einstein condensate and the orthogonality catastrophe, Phys. Rev. A 103, 013317 (2021).
- [14] N. B. Jørgensen, L. Wacker, K. T. Skalmstang, M. M. Parish, J. Levinsen, R. S. Christensen, G. M. Bruun, and J. J. Arlt, Observation of Attractive and Repulsive Polarons in a Bose– Einstein Condensate, Phys. Rev. Lett. 117, 055302 (2016).
- [15] M.-G. Hu, M. J. Van de Graaff, D. Kedar, J. P. Corson, E. A. Cornell, and D. S. Jin, Bose Polarons in the Strongly Interacting Regime, Phys. Rev. Lett. 117, 055301 (2016).
- [16] J. Etrych, G. Martirosyan, A. Cao, C. J. Ho, Z. Hadzibabic, and C. Eigen, Universal Quantum Dynamics of Bose Polarons, Phys. Rev. X 15, 021070 (2025).
- [17] N.-E. Guenther, P. Massignan, M. Lewenstein, and G. M. Bruun, Bose polarons at finite temperature and strong coupling, Phys. Rev. Lett. 120, 050405 (2018).
- [18] V. Pastukhov, Polaron in the dilute critical Bose condensate, J. Phys. A: Math. Theor. 51, 195003 (2018).
- [19] D. Dzsotjan, R. Schmidt, and M. Fleischhauer, Dynamical Variational Approach to Bose Polarons at Finite Temperatures, Phys. Rev. Lett. 124, 223401 (2020).
- [20] B. Field, J. Levinsen, and M. M. Parish, Fate of the Bose polaron at finite temperature, Phys. Rev. A 101, 013623 (2020).
- [21] G. Pascual and J. Boronat, Quasiparticle Nature of the Bose Polaron at Finite Temperature, Phys. Rev. Lett. 127, 205301 (2021).
- [22] M. Drescher, M. Salmhofer, and T. Enss, Bosonic functional determinant approach and its application to polaron spectra, Phys. Rev. A 110, 063303 (2024).
- [23] Z. Z. Yan, Y. Ni, C. Robens, and M. W. Zwierlein, Bose polarons near quantum criticality, Science **368**, 190 (2020).
- [24] A. L. Gaunt, T. F. Schmidutz, I. Gotlibovych, R. P. Smith, and Z. Hadzibabic, Bose–Einstein Condensation of Atoms in a Uniform Potential, Phys. Rev. Lett. 110, 200406 (2013).
- [25] C. Eigen, A. L. Gaunt, A. Suleymanzade, N. Navon, Z. Hadzibabic, and R. P. Smith, Observation of Weak Collapse in a Bose–Einstein Condensate, Phys. Rev. X 6, 041058 (2016).
- [26] N. Navon, R. P. Smith, and Z. Hadzibabic, Quantum gases in optical boxes, Nat. Phys. 17, 1334 (2021).
- [27] To avoid trapping atoms outside of the optical box, we always start our measurements with a quasipure BEC in a shallow trap of depth $U_D \approx k_B \times 50$ nK. We then raise the depth to $U_D \approx k_B \times 1$ µK, inject energy by sinusoidally forcing the

- system using a magnetic field gradient, and allow the gas to rethermalize at $a_b \approx 100a_0$.
- [28] To minimize Fourier broadening and stay in the linear response regime, here we use pulse durations $t_{rf} = \{0.8-6.4\}$ ms and always limit the injection fractions to $\lesssim 10\%$.
- [29] M. Drescher, M. Salmhofer, and T. Enss, Quench Dynamics of the Ideal Bose Polaron at Zero and Nonzero Temperatures, Phys. Rev. A 103, 033317 (2021).
- [30] Note that in the ideal-polaron theory, the spectra are expected to evolve continuously as the bath temperature is increased, with no sharp change at T_c, and we have experimentally checked that the injection spectra do not qualitatively change just below T_c.
- [31] See Supplemental Material for details on the effects of nonzero *T* for impurities in a BEC, further data on spectral shifts in the regime of weak interactions, and comparison between the ideal-polaron and two-body theory at high *T*.
- [32] J. Levinsen, L. A. Peña Ardila, S. M. Yoshida, and M. M. Parish, Quantum Behavior of a Heavy Impurity Strongly Coupled to a Bose Gas, Phys. Rev. Lett. 127, 033401 (2021).
- [33] A. Y. Chuang, H. Q. Bui, A. Christianen, Y. Zhang, Y. Ni, D. Ahmed-Braun, C. Robens, and M. Zwierlein, Observation of a Halo Trimer in an Ultracold Bose–Fermi Mixture, Phys. Rev. X 15, 021098 (2025).
- [34] B. Mukherjee, P. B. Patel, Z. Yan, R. J. Fletcher, J. Struck, and M. W. Zwierlein, Spectral Response and Contact of the Unitary Fermi Gas, Phys. Rev. Lett. 122, 203402 (2019).
- [35] We always correct Γ for residual Fourier broadening arising from our finite rf-pulse times, $t_{\rm rf}$, using $\Gamma = \left(\Gamma_{\rm e}^2 \Gamma_{\rm t}^2\right)^{1/2}$, where $\Gamma_{\rm e}$ is the raw extracted width and $\Gamma_{\rm t} \approx 2.78/t_{\rm rf}$ is the width of our response function [16].
- [36] D. M. Harber, H. J. Lewandowski, J. M. McGuirk, and E. A. Cornell, Effect of cold collisions on spin coherence and resonance shifts in a magnetically trapped ultracold gas, Phys. Rev. A 66, 053616 (2002).
- [37] M. W. Zwierlein, Z. Hadzibabic, S. Gupta, and W. Ketterle, Spectroscopic Insensitivity to Cold Collisions in a Two-State Mixture of Fermions, Phys. Rev. Lett. 91, 250404 (2003).
- [38] R. Lopes, C. Eigen, N. Navon, D. Clément, R. P. Smith, and Z. Hadzibabic, Quantum Depletion of a Homogeneous Bose-Einstein Condensate, Phys. Rev. Lett. 119, 190404 (2017).
- [39] Note that similar conclusions were obtained in interferometric experiments with single-component Bose gases [43]; for $n\lambda^3 = 0.13$ ($T/T_c \approx 7$) the measurements were consistent with the two-body theory, but measurements for $n\lambda^3 = 0.54$ ($T/T_c \approx 3$) revealed effects of three-body correlations.
- [40] M. Sun, H. Zhai, and X. Cui, Visualizing the Efimov Correlation in Bose Polarons, Phys. Rev. Lett. 119, 013401 (2017).
- [41] A. Christianen, J. I. Cirac, and R. Schmidt, Phase diagram for strong-coupling Bose polarons, SciPost Phys. 16, 067 (2024).
- [42] T. A. Hilker, L. H. Dogra, C. Eigen, J. A. P. Glidden, R. P. Smith, and Z. Hadzibabic, First and Second Sound in a Compressible 3D Bose Fluid, Phys. Rev. Lett. 128, 223601 (2022).
- [43] R. J. Fletcher, R. Lopes, J. Man, N. Navon, R. P. Smith, M. W. Zwierlein, and Z. Hadzibabic, Two- and three-body contacts in the unitary Bose gas, Science 355, 377 (2017).

SUPPLEMENTAL MATERIAL

Effect of nonzero T for impurities in a BEC

Initially, our quasipure BEC has $T \approx 10\,\mathrm{nK}$ [38] such that $T/T_\mathrm{c} < 0.1$, but both the impurities and the bath can be excited during injection, due to dynamics arising from inhomogeneity near the box edges and due to three-body losses. The effect of such excitations should be similar to that of a nonzero initial T, and for the theory comparisons in Figs. 1 and 2, we used $T/T_\mathrm{c} = 0.15$.

In Fig. S1, we illustrate the effect of such small nonzero T in the theory (see also [22]). We plot the ideal-polaron theory for T=0 and for different small $T/T_{\rm c}$, alongside our BEC data. The theoretical $E_{\rm p}$ values for the repulsive branch show only small variation with T, while $|E_{\rm p}|$ of the attractive branch for $-1\lesssim 1/(k_na)\lesssim 0$ is suppressed with increasing T. For $1/(k_n|a|)\gtrsim 1$, the theoretical Γ is very small only for T=0, and any small T causes significant broadening. On the other hand, near $1/(k_na)\approx 0$, Γ changes only slowly with T. We find that an effective $T/T_{\rm c}=0.15$ captures the data reasonably well for all $1/(k_na)$.

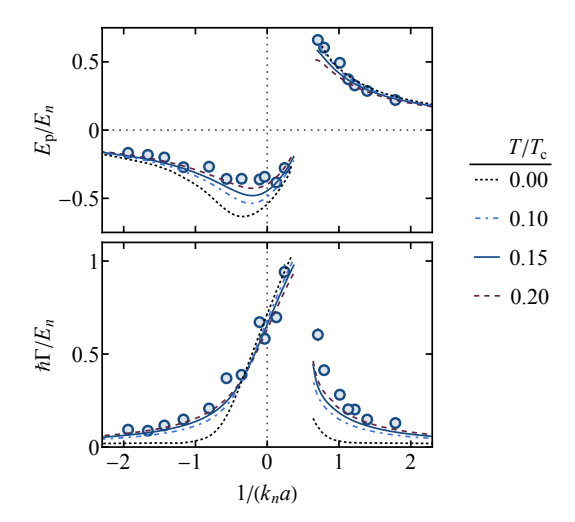


FIG. S1. Comparison of our BEC-bath data [16] with the ideal-polaron theory at zero and nonzero T. Plot of E_p/E_n (top) and $\hbar\Gamma/E_n$ (bottom) versus $1/(k_na)$, showing the data (symbols) and the ideal-polaron theory at different T/T_c (legend).

Spectral shifts in the weakly interacting regime

In Fig. S2, we show our measured $E_{\rm p}$ values for low a, where spectral shifts reflect the mean-field impurity energy $E_{\rm mf} = 2\pi\hbar^2\alpha na/m_{\rm r}$. For our BEC data [16], we used such measurements to calibrate the bath density; for our thermal baths, we instead calculate the density using the independently measured V and atom number N.

For injection spectroscopy of a thermal gas, one expects $\alpha=2$, reflecting the enhanced probability of finding two identical bosons on top of each other in the initial single-component gas [36, 37]; for a BEC, on the other hand, $\alpha=1$. However, as shown in Fig. 2, we find $\alpha=1.1(4)$, with the error dominated by our systematic uncertainties in N

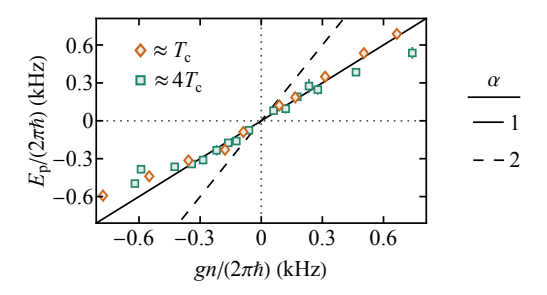


FIG. S2. Mean-field energy shift in the weakly interacting regime. Spectrum mode E_p versus gn, where $g = 2\pi\hbar^2 a/m_r$. The solid and dashed lines show $E_p = \alpha gn$ with, respectively, $\alpha = 1$ and 2 (see text for details).

and V. Experimentally, the measured α should be slightly lower than 2 due to the nonzero fraction of transferred impurities, but since our transfer fractions are $\lesssim 10\%$, this explains only a small part of the discrepancy.

When comparing our data with the two-body theory in Fig. 3, we extract $E_0 = E_{\rm mf} \lambda / a$ from the slope of $E_{\rm p}$ versus a for $a/\lambda \ll 1$.

Ideal-polaron theory for $T/T_c \gg 1$

In Fig. S3, we compare $E_{\rm p}$ and Γ in the ideal-polaron model to the high-T two-body theory, in which $E_{\rm p} - i\hbar\Gamma = -2\pi\hbar^2\alpha nf(a)/m_{\rm r}$, where

$$f(a) = -\left(\frac{m}{m_{\rm r}}\right)^{3/2} \frac{\lambda^3}{(2\pi)^3} \int \frac{a}{1 + ika} \exp\left(-\frac{\hbar^2 k^2}{2m_{\rm r}k_{\rm B}T}\right) {\rm d}^3 \mathbf{k}$$
(S1)

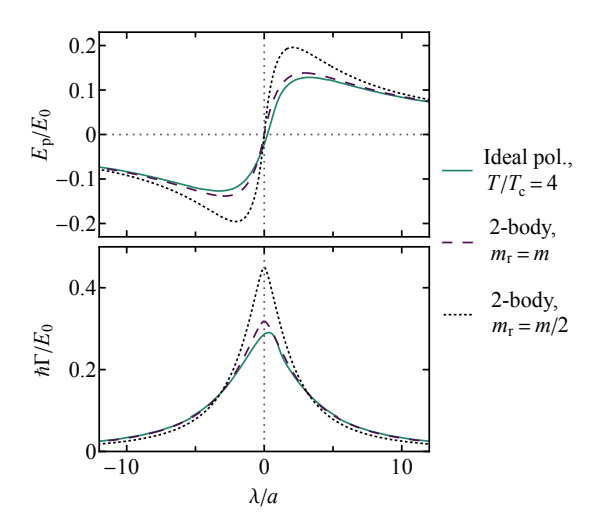


FIG. S3. Approaching the Boltzmann-gas regime in the ideal-polaron model. Spectrum mode E_p/E_0 (top) and half-width-at-half-maximum $\hbar\Gamma/E_0$ (bottom) obtained from the ideal-polaron FDA calculations and the high-T two-body approximation (see legend and text for details).

is the thermally averaged scattering amplitude. More explicitly, one obtains:

$$\frac{E_{\rm p}}{E_0} = \frac{v}{\sqrt{\pi}} \left[1 - \sqrt{\pi} |v| \exp(v^2) \operatorname{erfc}(|v|) \right] \sqrt{\frac{m}{m_{\rm r}}}, \quad (S2)$$

$$\frac{\hbar\Gamma}{E_0} = \frac{1}{\pi} \left[1 + v^2 \exp(v^2) \operatorname{Ei}(-v^2) \right] \sqrt{\frac{m}{m_{\rm r}}},$$
(S3)

where we have introduced the scaled interaction parameter $v = \sqrt{m/(4\pi m_{\rm T})} \, \lambda/a$ and Ei(x) denotes the exponential integral; note that here m is the bath-atom mass and $m_{\rm T}$ is the

reduced mass of an impurity and a bath atom.

For our highest $T/T_{\rm c}$, the ideal-polaron predictions (green solid lines) are already close to the two-body theory with $m_{\rm r}=m$ (dashed line), demonstrating that many-body effects become essentially irrelevant for T well above $T_{\rm c}$. Note that unlike the full ideal-polaron FDA calculations, the two-body theory can be easily extended to the equal-mass case with $m_{\rm r}=m/2$ (dotted line, same as the solid line in Fig. 3); the additional dependence on $m/m_{\rm r}$ explains some of the difference between the ideal-polaron theory and the experimental data for our highest $T/T_{\rm c}\approx 4$.